A New Approach to Gravitational Gradient Determination of the Vertical

JOHN W. DIESEL*
Litton Systems, Inc., Beverly Hills, Calif.

A new technique is described for accurately determining the vertical from orbiting vehicles. Although the gravitational gradient phenomenon on which it is based is already well known, previously proposed devices based on this effect are impractical because of inherent accelerometer errors and extraneous vehicle motion that would disturb the accelerometer case. The new approach described herein bypasses both of these problems. The proposed system is unaffected by bias and scale factor errors and senses only the desired gravitational differences even when not in free fall. To explain the approach, a general theory of the gravitational gradient effect is presented. It is shown that the directions defined by this effect are the eigenvectors of a second-rank tensor. These eigenvectors are then determined for the earth's gravitational field, and a simple new method of finding the gravitational torques on rigid bodies is presented. Finally, some general results are obtained regarding the effect of the gravitational gradient on the constrained motion of rigid bodies such as would be used in this approach.

THE gravitational gradient phenomenon has frequently been discussed as a means of determining the vertical from orbiting vehicles.[1, 2] But the conventionally proposed approach has remained of only academic interest because of the apparently insurmountable instrumentation problems involved. A new approach described herein bypasses the worst of these problems so that a new look at this phenomenon appears to be justified.

The importance of an accurate vertical reference in orbiting vehicles may be appreciated by observing that the accuracy of a self-contained navigation system is limited by the precision with which the vertical can be established. Although present needs for accurate navigation have been met by line-of-sight tracking and communication links with the ground, the operational flexibility of future manned, maneuverable space vehicles would be severely limited by such a system. In cases where self-contained navigation is essential, the vertical can be established by horizon scanners that are already in an advanced state of hardware development. But such instruments will always be limited in accuracy by variations in the physical horizon itself which may cause uncertainties of 0.1° or more at low altitudes.[3] On the other hand, uncertainties in the gravitational gradient effect should be as low as 0.01 mrad (2 sec of arc) in most cases, so that an instrument that could exploit this potential accuracy would be highly desirable.

The present paper describes a new method for accurately determining the vertical from the gravitational gradient effect. Although many excellent papers have explained the theory of this phenomenon as it relates to special applications,[2, 7] these are not sufficiently general to describe the new approach. A general theory of this effect is, therefore, presented herein. In particular, it is shown that the tangential variation of gravitation around a circle is almost purely sinusoidal despite anomalies in the field. This phenomenon permits accurate determination of the vertical despite accelerometer-bias and scale-factor errors and extraneous noise. Also, by considering the gravitational gradient torques on the constrained motion of a rigid body, it is shown that the desired gravitational gradient effect can be sensed without sensing extraneous vibrations and disturbing accelerations even when not in free fall.

Received May 23, 1963; revision received December 9, 1963.

* Member of the Senior Technical Staff, Guidance and Control Systems Division. Member AIAA.

Basic Principles

Gravitational gradient devices for determining the vertical operate by measuring or detecting small differences in the gravitational field from one point to another. This section discusses the nature of these differences, how they are detected, and how the observed differences might be used to determine the vertical.

The gravitational field due to an approximately spherical mass such as the earth is as shown in Fig. 1a. Gravitation $\mathbf{G}$ at points $\mathbf{R}$ near a reference point O differs from gravitation, $\mathbf{G}_0$, at O by the difference $\mathbf{g} = \mathbf{G} - \mathbf{G}_0$ shown in Fig. 1b. The tangential component g_θ of this difference at points on a circle of radius r about O is shown in Fig. 1c. It is observed that this component varies sinusoidally with angular position θ around the circle and completes 2 cycles/revolution in θ. The magnitude of this variation is of the order of 0.5×10^{-7} g/ft radius of the circle at the usual orbital altitudes. It is clear from Fig. 1 that the vertical can be determined as one of

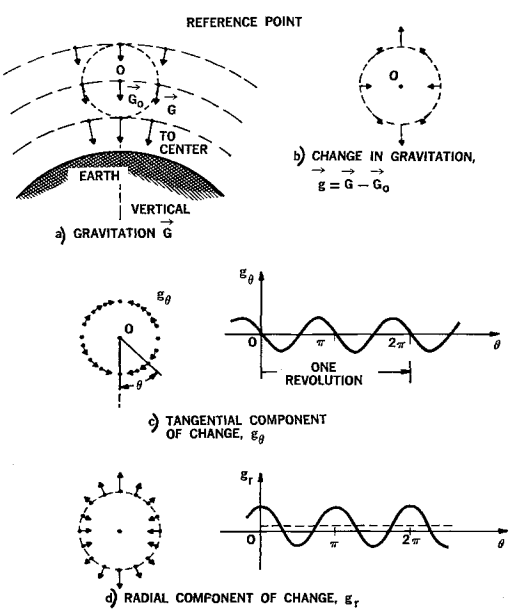

Fig. 1 Gravitational field near a reference point over earth.

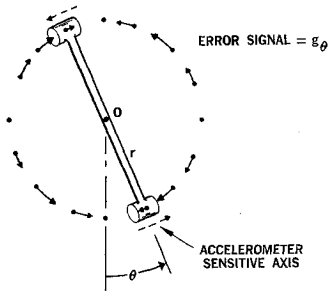

Fig. 2 Conventional approach to determine the vertical.

the directions for which this sinusoid goes through zero. As shown in Fig. 1d, the radial component of **g** also varies sinusoidally, with a d.c. component, and reaches its maximum value in the direction of the vertical. In the next section it is shown that these directions are defined by the eigenvectors of the gravitational gradient tensor. It is also shown that these directions are not, in general, the same as the direction of gravitation when the field is not central. But, the variation in g_θ will be sinusoidal.

Although the foregoing effect would always exists at various points within a vehicle, it is ordinarily not observable when the vehicle is within the atmosphere because the effect represents an extremely small part of the total gravitational field. But in orbiting vehicles, the effect becomes conspicuous. If point O is in free fall, an accelerometer at O measures $\ddot{\mathbf{R}}_0 - \mathbf{G}_0 = 0$. An accelerometer at a nearby point, whose acceleration with respect to O is $\ddot{\mathbf{r}}$, will measure

$$(\ddot{\mathbf{R}}_0 + \ddot{\mathbf{r}}) - (\mathbf{G}_0 + \mathbf{g}) = \ddot{\mathbf{r}} - \mathbf{g}$$

If the vehicle is not rotating, $\ddot{\mathbf{r}} = 0$, and such an accelerometer measures only the desired gravitational difference, $-\mathbf{g}$. Since these ideal conditions will not be encountered in an actual vehicle, the accelerometer will measure additional disturbance accelerations. In the conventional approach, several accelerometers are used to obtain additional measurements from which $-\mathbf{g}$ can be computed.

Figure 2 typifies the conventionally proposed approach. The outputs of the accelerometer pair are summed, and this sum is used as an error signal to rotate the device toward the vertical where the error signal is thus nulled. For a device of radius 1 ft, this signal is of the order 10^{-11} g/0.1-mil error from the vertical. That is, an accelerometer bias error of only 10^{-11} g would cause a 0.1-mil error in the vertical. In addition, each accelerometer must measure accelerations of the vehicle to this same precision so that such accelerations exactly cancel in the summation to obtain the error signal. Such accuracy is far beyond the present state of the art because of the accelerometer bias and scale factor errors. Even if a suitable accelerometer could be developed, extraneous noise due to structural compliance and vibrations of the vehicle would almost certainly swamp out the effect to be measured. That is, because of disturbances, even a perfect accelerometer would not measure just the desired signal $-g_\theta$ shown in Fig. 1c. Although modifications of this device have been proposed, they all suffer essentially these same disadvantages. The various approaches are described in Ref. 3, and the effect of errors are discussed by Roberson.[4]

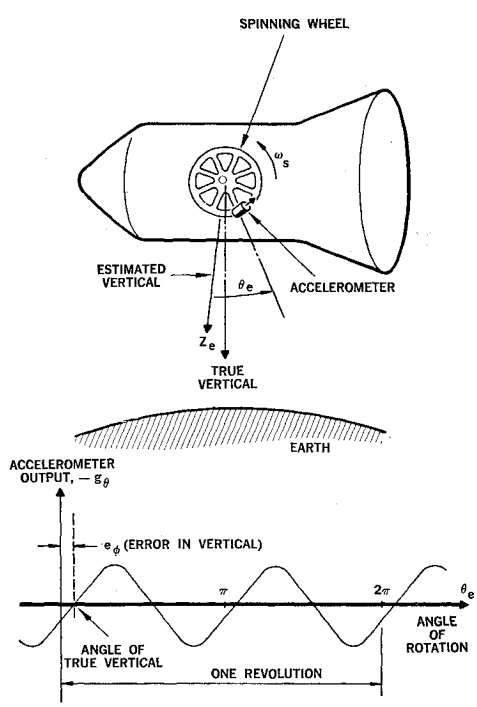

Fig. 3 Vertical indicating system.

A new approach, which bypasses both these problems, will now be explained. First, it will be observed that a single accelerometer rotated at a constant angular rate as suggested in Fig. 3 would sense the sinusoidal variation of g_θ. The vertical is then defined by the phase of this signal. As will be shown subsequently, the wheel speed need not be accurately controlled. One advantage of this approach over the conventional approach typified in Fig. 2 is obvious; since the same accelerometer is used in Fig. 3 to detect g_θ at various points around the circle, bias errors and scale factor errors will exactly cancel when determining the phase angle e_ϕ, which defines the vertical. Thus, the need for carefully matched pairs of accelerometers is avoided. A further description of this system is given in Ref. 5.

The phase error indicated in Fig. 3 can be readily detected by continuously resolving the accelerometer output through angle $2\theta_e$. The resolver rotor moves with the spinning wheel, whereas the stator is relatively stationary and is fixed to the axis Z_e representing the estimated vertical. As shown in Fig. 4a, the resolved signal will, in general, have a d.c. component and a ripple at twice the frequency of g_θ. Clearly, the d.c. component represents the phase error e_ϕ, which is the error in the vertical. It is then desirable to detect this d.c. component and reject the ripple. The detected d.c. component e_ϕ is then used to slowly turn the resolver stator, and hence the estimated vertical axis Z_e, until the error in the vertical is nulled.

In order to reject the ripple, the resolved signal is integrated over N complete revolutions of the wheel. The result is just the desired error signal:

$$e_\vartheta = \frac{1}{2\pi N}\int_0^{2\pi N} -\sin 2\theta \cos 2\theta_e d\theta \qquad (1)$$

This is achieved by an integration in real time over a finite interval T, which is a multiple N of the time T_s required for the cosine resolver to complete one revolution. One way to perform this finite memory integration is to use an ordinary integrator followed by a sampling switch of period T_s connected between the resolver rotor and stator. The finite integration is then obtained by subtracting successive samples of the integrator output as shown in Fig. 4b. These operations eliminate the ripple as well as other noise and disturbance signals in the system.

The use of the error signal e_ϕ in a closed loop vertical tracking system is indicated in Fig. 5. Two integrations are included in the loop to avoid steady-state errors due to the orbital angular velocity of the true vertical. The effect of the phase error detector is to introduce the transfer function $(1 - e^{-Ts})/Ts$. Lead compensation is clearly required for stability, as indicated by the Nyquist diagram of Fig. 5.

Because of the slow angular frequency $\dot{\phi}$ of the true vertical, the desired signal g_θ has frequency $2\omega' = 2(\omega_s - \dot{\phi})$, which differs slightly from $2\omega_s$. The manner in which the phase error detector rejects all other frequencies is indicated in Fig.

6, which was obtained by analyzing Eq. (1). As indicated, the phase error detector is effectively an extremely narrow band pass filter that drastically attenuates all signals except those at the desired signal frequency $2\omega'$. The bandwidth of this filter is proportional to $1/N$, where N is the ratio of the total integration time T to the period T_s of the wheel. For most orbital applications, the angular rate $\dot{\phi}$ of the true vertical cannot change suddenly, so that a very narrow bandwidth, about $2\omega'$, will pass the desired signal frequencies.

It is important to observe that accelerometer bias errors appear at nearly zero frequency. Also, the fraction of centripetal acceleration which was picked up because of sensitive axis misalignment will appear at zero frequency. As shown in Fig. 6, these zero-frequency terms will be eliminated in the system output. Also, if the reference point O is not in free fall, the difference $\ddot{\mathbf{R}}_0 - \mathbf{G}_0$ will appear as a sinusoid at frequency ω' and will be eliminated in the output. Similarly, accelerometer scale factor errors, which cause harmonics of the signal g_θ at frequencies $4\omega'$, $8\omega'$, etc., will be eliminated.

The sources of error that are not eliminated are those that appear at frequencies very near the frequency $2\omega'$ of the signal g_θ. One such error will result from detecting the radial component g_r of Fig. 1d because of misalignment of the accelerometer sensitive axis. A 1-mrad misalignment error causes a $\frac{1}{2}$-mrad error in the vertical. Another source of error is random noise power that appears at frequency $2\omega'$. Analysis of Eq. (1) shows that the total output power due to such noise is

$$P_{\text{out}} = (\pi/T)\Phi_N(2\omega') \qquad (2)$$

where $\Phi_N(2\omega')$ is the level of the noise power spectral density at frequency $2\omega'$. It is clear that an accelerometer designed for this application should have a very low noise level or "window" in its noise power spectrum at some frequency $2\omega'$. The frequency of rotation ω_s should then be chosen so that $2\omega'$ occurs at this frequency. Additional random noise will occur at frequency $2\omega'$ because of 1) variation in the angular velocity of the wheel, and 2) undesired translational acceleration of reference point O when the center of the wheel is not in free fall. The geometry of the wheel bearings and drive motor should be selected so that angular velocity variations 1 are not harmonically related to the wheel speed.

By means of a flexure suspension system, the angular variations in rate of rotation can be made to almost exactly cancel the translational acceleration of reference point O so that noise sources 1 and 2 do not disturb the system. For example, consider an accelerometer mounted to a freely rotating double-bob pendulum so that the accelerometer axis is in the angular direction shown in Fig. 7, and assume that the pivot undergoes a disturbance acceleration $\delta\ddot{\mathbf{R}}_0 = \ddot{\mathbf{R}}_0 - \mathbf{G}_0$. Even though the pivot is not in free fall, the accelerometer will not sense the disturbance, since angular accelerations of the pendulum exactly cancel the component of $\delta\ddot{\mathbf{R}}_0$ along the accelerometer sensitive axis. The gravitational gradient signal g_θ is not similarly canceled, since the mass of the bob is concentrated at two points 90° apart in space and hence 180° apart with respect to the double-frequency sinusoidal signal g_θ. Thus, the pendulum and accelerometer case are not accelerated by g_θ, and the accelerometer detects this signal. To maintain the average angular rate ω_s, the pendulum is mounted with its pivot along the axis of a spinning wheel with counterbalance. Limited freedom of angular motion is provided by a flexure pivot with a natural frequency that is small compared to the angular frequency of rotation, so that the pendulum is relatively free to isolate the accelerometer from disturbance accelerations; yet the accelerometer remains close to a nominal angular position with respect to the spinning wheel. Such a device should be usable in orbital systems even though atmospheric drag, low-thrust engines, or other disturbances create accelerations $\delta\ddot{\mathbf{R}}_0$ considerably different from zero. It is emphasized here that this device is not a rotating pendulous accelerometer (e.g., Ref. 6).

In the next sections, the foregoing intuitive discussions will be verified by examining the theory of the gravitational gradient phenomenon and its effect on the constrained motion of rigid bodies. A preliminary error analysis is then presented together with typical values of the parameters.

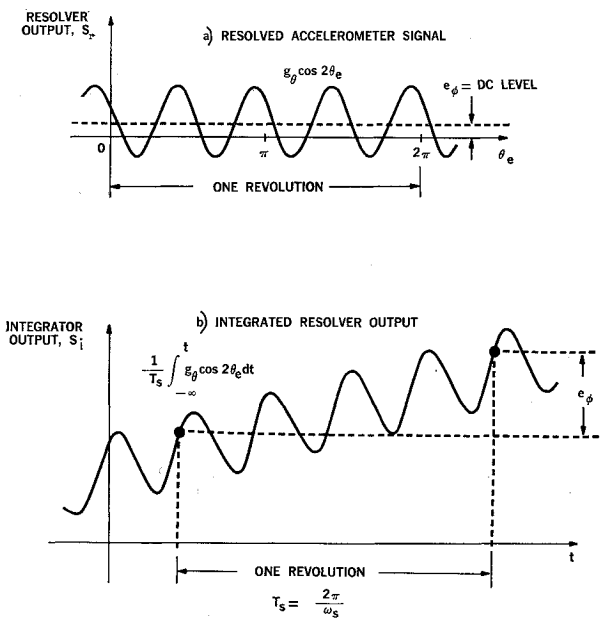

Fig. 4 Detection of phase error.

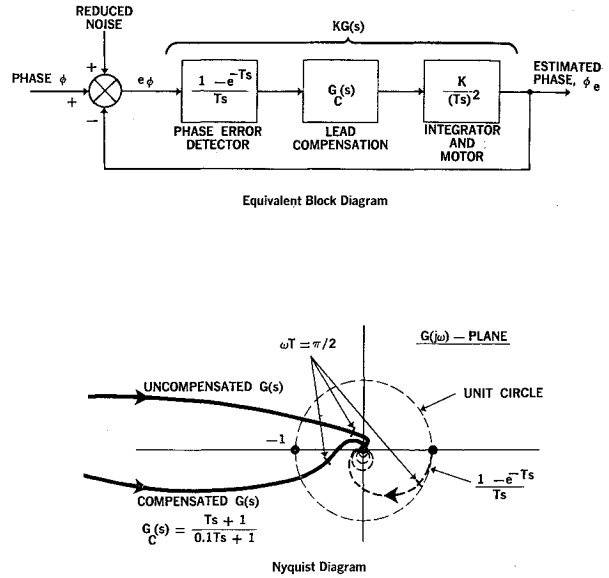

Fig. 5 A possible closed loop phase tracking system.

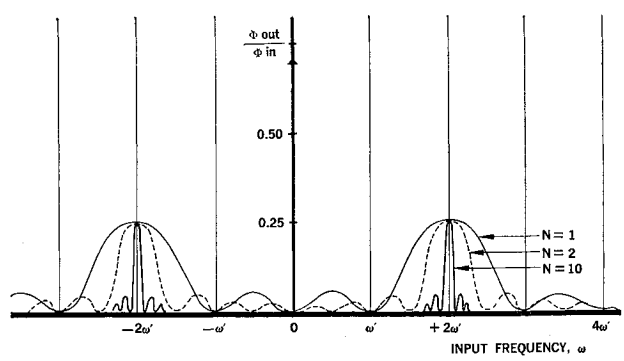

Fig. 6 Power density attenuation vs input frequency.

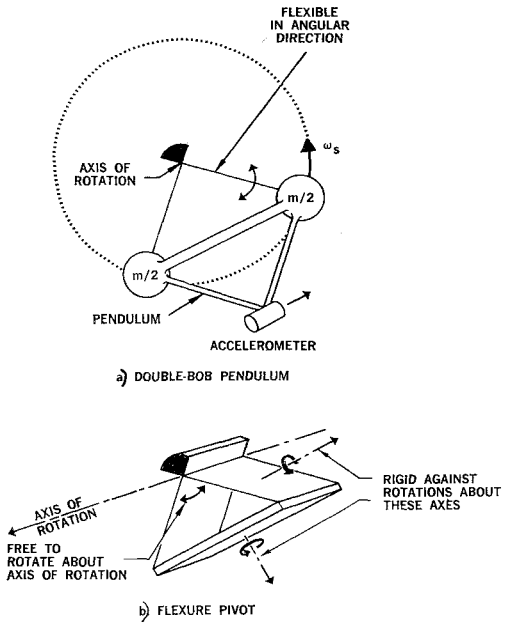

Fig. 7 Gravitational gradient detector.

Theory

Second-Rank Tensors of the Gravitational Field

As has been shown in Refs. 7 and 8, the gravitational differences **g** about a reference point O are given to an extremely high accuracy (error less than 10^{-14} g/ft for earth satellites) by the first-order terms in the Taylor expansion of **G** about O. That is, in a rectangular coordinate system with axes 1, 2, 3, the components g_i of **g** are given as linear functions of the coordinates r_i of the displacement from O. If V (**R**) is the gravitational potential function at position **R**, then $g_i = \Sigma_j V_{ij} r_j$, where $V_{ij} = \partial^2 V/\partial R_i \partial R_j$ evaluated at O. In matrix notation,

$$g] = [V]r] \tag{3}$$

If the 1, 2 axes define the plane of a circle of radius r about O, then the components of **g** in the tangential, radial, and normal directions can be expressed in polar coordinates by taking the dot product of (3) with the unit polar coordinate vectors $\mathbf{U}_\theta$, $\mathbf{U}_r$, $\mathbf{U}_0$, with the result

$$\begin{aligned} g_\theta &= (r/2)\{(V_{22} - V_{11}) \sin 2\theta + 2V_{12} \cos 2\theta\} \\ g_r &= (r/2)\{-(V_{22} - V_{11}) \cos 2\theta + 2V_{12} \sin 2\theta + \\ &\qquad (V_{22} + V_{11})\} \\ g_0 &= r\{V_{13} \cos\theta + V_{23} \sin\theta\} \end{aligned} \tag{4}$$

It is obvious that these variations are exactly sinusoidal within the accuracy of Eq. (3) even though the gravitational field is not central and the plane of rotation is arbitrary. However, these expressions are further simplified if a coordinate system can be found in which the off-diagonal elements of $[V]$ vanish so that the phase angles in Eq. (4) are zero. Equation (4) then describes quantitatively the variations shown in Fig. 1.

In a new coordinate system 1′, 2′, 3′, the coordinates g_i', of **g** and r_j' of **r** are related by

$$g'] = [V']r'] \tag{3'}$$

where $[V']$ is the square matrix of second partial derivatives $V_{ij}' = \partial^2 V/\partial R_i' \partial R_j'$. Corresponding quantities in Eqs. (3) and (3′) satisfy tensor relationships $g'] = [A]g]$, $r'] = [A]r]$, and $[V'] = [A][V][A]_t$, where $[A]$ is the orthogonal transformation matrix from the unprimed to the primed system and $[A]_t$ is its transpose. The differentiability of V insures that V_{ij} is real and that $V_{ij} = V_{ji}$. Thus, $[V]$ is a real symmetric matrix; the gravitational gradient tensor is then said to be self-adjoint or "hermitean." A property of such tensors is that the eigenvectors are always real and orthogonal.[9] Therefore, there exists an orthogonal transformation $[A]$ such that, in the new coordinate system, $[V']$ is diagonal:

$$[V'] = \begin{bmatrix} \lambda_1 & 0 & 0 \\ 0 & \lambda_2 & 0 \\ 0 & 0 & \lambda_3 \end{bmatrix} \tag{5}$$

The unit vectors $\mathbf{U}_i'$ defining this system are the unit eigenvectors of $[V]$, and the λ_i are the eigenvalues. It is shown subsequently that the torque on a rigid body due to the gravitational gradient vanishes when the principle body axes are aligned with these vectors. These are also the directions determined by gravitational gradient devices for indicating the vertical.

Finally, it should be observed that the foregoing eigenvectors and, hence, the directions sensed by gravitational gradient devices are not determined by the direction of gravitation. For if a uniform field is superimposed on a field with gravitation **G** and gravitational gradient $[V]$, the direction of gravitation is clearly changed, although the gravitational gradient is not affected.

The eigenvectors will now be found for the earth's gravitational field. When the gravitational potential function V is expressed in the usual spherical harmonic expansion, the predominant terms are the central force term V_{00} and the bulge term V_{20} due to earth's rotation. Then $V \cong V_{00} + V_{20}$ where

$$\begin{aligned} V_{00} &= kM/R \\ V_{20} &= (kM/R)J_{20}(R_e/R)^2 P_{20}(\sin\upsilon) \end{aligned} \tag{6}$$

Here υ is latitude, R/R_e is a normalized radius, P_{20} (sinυ) is the associated Legendre polynomial of the first kind of degree 2 and order 0, kM is the Newtonian gravitational constant times the mass of the earth, and the bulge coefficient $J_{20} \cong -10^{-3}$. Although a direct evaluation of the eigenvectors of Eq. (6) would be an extremely formidable problem, the eigenvectors can be found for each term separately and the results combined using small-angle approximations. After considerable reduction, the eigenvectors are found to lie along the X'', Y'', Z'' axes shown in Fig. 8. These axes are tilted with respect to the geocentric vertical axis by an angle

$$\delta = -2J_{20}(R_e/R)^2 \sin 2\upsilon \tag{7}$$

which is twice the corresponding tilt of the gravitational vector itself. In these coordinates, the gravitational gradient tensor is given by

$$[V''] = \omega_g^2 \begin{bmatrix} \frac{2}{3} + \epsilon_{11} & 0 & 0 \\ 0 & \frac{1}{3} + \epsilon_{22} & 0 \\ 0 & 0 & -\frac{1}{2} + \epsilon_{33} \end{bmatrix} \tag{8}$$

where

$$\begin{aligned} \epsilon_{11} &= J_{20}(R_e/R)^2(1 - 3\cos 2\upsilon) \\ \epsilon_{22} &= J_{20}(R_e/R)^2 \tfrac{1}{4}(5\cos 2\upsilon - 3) \\ \epsilon_{33} &= J_{20}(R_e/R)^2 \tfrac{1}{4}(7\cos 2\upsilon - 1) \end{aligned} \tag{9}$$

and ω_g^2 is given by

$$\omega_g^2 = 3kM/R^3 \tag{10}$$

In Eq. (8), terms of order ϵ^2 were neglected since $\epsilon_{ii} < 4 \times 10^{-3}$ from Eq. (9). The quantity ω_g is recognized as the angular frequency of small-angle dumbell oscillation of a satellite about the vertical.

Gravitational Gradient Torques on a Rigid Body

Although expressions for the gravitational gradient torques on a rigid body have been presented elsewhere,[8] the form of

these expressions is primarily useful when considering the small-angle oscillations of a satellite about a nominal attitude. In order to study the gravitational effect on the constrained motion of rigid bodies, such as the double-bob pendulum described herein, it is desirable to derive the torque expressions in a different form. The results are easily derived and are presented in Eqs. (12–14) below. These expressions are extremely simple and involve only the eigenvalues of the gravitational gradient tensor and the eigenvalues of the body inertia tensor $[I]$ with respect to a reference point O. Since they are applicable to any gravitational field and any rigid body, and do not depend on small-angle approximations, the results are of general theoretical interest.

The first result to be obtained is that, with respect to O, the torque $\mathbf{q}$ due to the gravitational change $\mathbf{g}$ is zero if the new† principal body axes $1', 2', 3'$, with respect to O, are aligned with the eigenvectors of $[V]$, even though the centroid is displaced from O in some arbitrary direction $\mathbf{r}_c$. The derivation here is quite simple. Denoting an element of mass of the body by dm_n and its position by $\mathbf{R}_n = \mathbf{R}_0 + \mathbf{r}_n$,

$$\mathbf{q} = \Sigma_n \mathbf{r}_n \times dm_n \mathbf{g}_n \tag{11}$$

where $\mathbf{g}_n$ is the gravitational change at particle n. If $\mathbf{U}_1$, $\mathbf{U}_2$, $\mathbf{U}_3$ are the unit eigenvectors of $[V]$, then $\mathbf{r}_n = \Sigma_i (r_n)_i \mathbf{U}_i$ and $\mathbf{g}_n = \Sigma_j \lambda_j (r_n)_j \mathbf{U}_j$. Substituting into the definition of $\mathbf{q}$, interchanging the order of summation between n and i, j, and using the definition of $[I]$,

$$\mathbf{q} = I_{23}(\lambda_2 - \lambda_3)\mathbf{U}_1 + I_{31}(\lambda_3 - \lambda_1)\mathbf{U}_2 + I_{12}(\lambda_1 - \lambda_2)\mathbf{U}_3 \tag{12}$$

The cross moments I_{ij} are taken with respect to the principal gravitational axis. If these are also principal body axes, then $I_{ij} = 0$ when $i \neq j$, by definition, so that $\mathbf{q} = 0$, which is the desired result.

When the principal body axes are not aligned with the principal gravitational axes, it is convenient to express $\mathbf{q}$ in terms of the fixed principal moments of inertia I_i in body axes. If the transformation from gravitational 1, 2, 3 to body axes $1', 2', 3'$ is represented by orthogonal matrix $[A]$, the I_{ij} can be expressed in terms of the I_i by the tensor transformation $[I] = [A]_t[I'][A]$, where $[I']$ is diagonal with elements I_i. The result is substituted into Eq. (12) to obtain

$$\mathbf{q} = \Sigma_i I_i\{(\lambda_2 - \lambda_3)a_{i2}a_{i3}\mathbf{U}_1 + (\lambda_3 - \lambda_1)a_{i3}a_{i1}\mathbf{U}_2 + (\lambda_1 - \lambda_2)a_{i1}a_{i2}\mathbf{U}_3\} \tag{13}$$

It is also convenient to express the torque in terms of its components along body axes $1', 2', 3'$. This is done by substituting $\mathbf{r} = \Sigma_i r_i' \mathbf{U}_i'$, $\mathbf{g} = \Sigma_j g_j' \mathbf{U}_j'$ into Eq. (11), with g_j' expressed in terms of r_j' by the usual relationship $g'] = [V']r']$. The result is

$$\mathbf{q} = \Sigma_j \lambda_j\{(I_2 - I_3)a_{2j}a_{3j}\mathbf{U}_1' + (I_3 - I_1)a_{3j}a_{1j}\mathbf{U}_2' + (I_1 - I_2)a_{1j}a_{2j}\mathbf{U}_3'\} \tag{14}$$

The Effect of the Gravitational Gradient on the Constrained Motion of Rigid Bodies

It will now be shown that a properly constrained rigid body, such as a double-bob pendulum rotating about the reference point O, undergoes such motion that an accelerometer suitably mounted to the body will detect only the desired gravitational differences g_θ independent of the motion of the reference point. The result is based on Lagrange's equation for the motion of a rigid body about fixed axis through moving point O.

† Observe the moment of inertia tensor $[I]$ is defined with respect to reference point O, which is not necessarily the centroid. Nevertheless, the symmetry of $[I]$ insures the existence of principal body axes and moments with respect to O, although these principal axes are not necessarily parallel to those about the centroid.

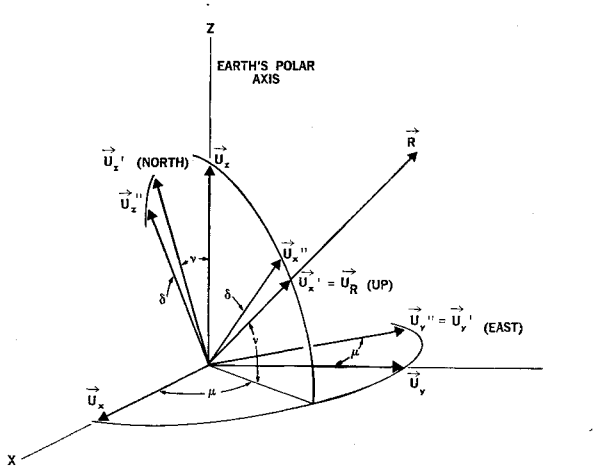

Fig. 8 Coordinates and eigenvectors of earth's gravitational field.

Let $\mathbf{U}_1$, $\mathbf{U}_2$, $\mathbf{U}_3$ be unit vectors defining an inertial coordinate system. Assume the axis of rotation is an axis $3'$ through point O and parallel to the fixed direction defined by $\mathbf{U}_3$. The motion about O is therefore two-dimensional and is represented by the generalized coordinate θ, the angle from inertial axes 1, 2 to body-fixed axes $1', 2'$, with respect to O. The generalized force Q_θ is the total gravitational torque about O defined by[9]

$$Q_\theta = \Sigma_n (dm_n \mathbf{G}_n) \cdot \partial \mathbf{R}_n / \partial \theta \tag{15}$$

whereas the total kinetic energy T of the body is defined by

$$T = \Sigma_n \tfrac{1}{2} dm_n \dot{\mathbf{R}}_n \cdot \dot{\mathbf{R}}_n \tag{16}$$

Lagrange's equation is then[9]

$$d/dt(\partial T/\partial \dot{\theta}) - (\partial T/\partial \theta) = Q_\theta \tag{17}$$

where Q_θ was used rather than $\partial V/\partial \theta$, since V depends on time due to the motion of O. As is customary, the dots denote time differentiation in inertial system 1, 2, 3.

With the usual definitions, $\mathbf{R}_n = \mathbf{R}_0 + \mathbf{r}_n$, $\mathbf{G}_n = \mathbf{G}_0 + \mathbf{g}_n$, the torque Q_θ is written as the sum of the torque Q_0 due to $\mathbf{G}_0$, and the torque q due to $\mathbf{g}$.

After some reduction of Eq. (15),

$$Q_0 = m\mathbf{G}_0 \cdot (\partial \mathbf{r}_c / \partial \theta) \tag{18}$$

In the usual case, the axis of rotation is a principal axis of the body, so that q is simply the component of the total torque $\mathbf{q}$ of the previous section along $\mathbf{U}_3'$, as given by Eq. (14):

$$q = \Sigma_j \lambda_j (I_1 - I_2) a_{1j} a_{2j} \tag{19}$$

It is observed that the torque q due to the gravitational gradient vanishes whenever $I_1 = I_2$. The expression for T can similarly be reduced to

$$T = \tfrac{1}{2} m \dot{\mathbf{R}}_0^2 + m\dot{\theta}\dot{\mathbf{R}}_0 \cdot (\partial \mathbf{r}_c / \partial \theta) + \tfrac{1}{2} I_{33} \dot{\theta}^2 \tag{20}$$

which shows the effect of the velocity $\dot{\mathbf{R}}_0$ of O and the displacement $\mathbf{r}_c$ of the centroid from O.

Substituting the simplified expressions Eqs. (18–20), Lagrange's equation becomes

$$m \cdot \delta \ddot{\mathbf{R}}_0 \cdot (\partial / \partial \theta) \mathbf{r}_c + I_{33} \ddot{\theta} = q \tag{21}$$

where $\delta \ddot{\mathbf{R}}_0 = \ddot{\mathbf{R}}_0 - \mathbf{G}_0$ indicates the departure of O from free fall. The first term is the sinusoidal component of $\delta \ddot{\mathbf{R}}_0$ along the rotating vector $\partial \mathbf{r}_c / \partial \theta$. It will vanish if O is in free fall so that $\delta \ddot{\mathbf{R}}_0 = 0$. Otherwise, it could be made to vanish by placing O at the centroid so that $\mathbf{r}_c = 0$. But this is undesirable, since this torque can be used to prevent the accelerometer from measuring disturbances. To this end, the accelerometer

is placed along the radial line to the centroid and with its sensitive axis in the direction of rotation. The polar coordinates of the accelerometer are denoted by r, θ and the corresponding unit vectors by $\mathbf{U}_r$, $\mathbf{U}_\theta$, so that $\mathbf{r}_c = r_c\mathbf{U}_r$, and the accelerometer sensitive axis is in the direction of $\mathbf{U}_\theta$. The accelerometer measures the dot product, $a_\theta = \{(\ddot{\mathbf{R}}_0 + \ddot{\mathbf{r}}) - (\mathbf{G}_0 + \mathbf{g})\}\cdot\mathbf{U}_\theta$. Substituting from Lagrange's equation and observing that $\ddot{\mathbf{r}}\cdot\mathbf{U}_\theta = r\ddot{\theta}$,

$$a_\theta = (r - \rho_{33}^2/r_c)\ddot{\theta} - g_\theta + (q/mr_c) \tag{22}$$

where ρ_{33} is the radius of gyration about the axis of rotation. Such an accelerometer will just measure $-g_\theta$ if the accelerometer is located a distance r from O given by

$$r = \rho_{33}^2/r_c$$

and if $I_1 = I_2$, so that the torque q given by Eq. (19) vanishes.

In summary, an accelerometer mounted to a rigid body free to rotate in a plane about point O in a vehicle will measure only the desired signal $-g_\theta$ independent of vehicle motion or gravitation, provided that 1) the principle body moments with respect to O are equal, and 2) the accelerometer and centroid are along the same radial line from O with $r = \rho_{33}^2/r_c$, and the sensitive axis is in the direction of rotation. The double-bob pendulum shown in Fig. 7 is one device that satisfies these requirements.

Error Analysis

Selection of System Parameters

A first consideration is the bandwidth required to provide fast reaction time and also small dynamic errors in tracking the vertical. Since conventional accelerometers and gyros are well suited to measuring velocity increments and attitude during major orbital adjustments, it will be assumed that the system is used only while the vehicle is in free fall or undergoing low accelerations due to drag or low thrust engines. In such cases the angle ϕ of the vertical will vary smoothly.

Dynamic errors will result from variations $\Delta\phi$ in the vertical which are not followed by the system because of bandwidth limitations. Consider first the error $\Delta\phi$ due to vehicle translational accelerations $R\ddot{\phi} = R\omega^2(\Delta\phi)_{\max}\cos\omega t$ at frequencies ω greater than the bandwidth ω_{BW}. The maximum error is $(\Delta\phi)_{\max} = (R\ddot{\phi})_{\max}/R\omega^2$. If $(R\ddot{\phi})_{\max} < 10^{-3}\ g$, the maximum error in the vertical, $(\Delta\phi)_{\max}$, will be less than 0.1 mrad provided $\omega_{BW} > 0.0124$ rad/sec. The corresponding integration time T must satisfy $T < 800$ sec. Next consider the steady-state error $(e_\phi)_{ss}$ due to a constant angular acceleration of the vertical $\ddot{\phi}$. Referring to Fig. 5, $(e_\phi)_{ss} = (T^2/K)\ddot{\phi}$, where, by suitable lag-lead compensation, a gain $K \geqq 10$ can be achieved. For orbits of low eccentricity e, the maximum angular acceleration is $\ddot{\phi}_{\max} \doteq 2e\omega_0^2$, where ω_0 is the orbital angular velocity. Assuming $\omega_0 = 10^{-3}$ rad/sec and $e = 0.1$, $\ddot{\phi}_{\max} = 2 \times 10^{-7}$ rad/sec^2, then $(e_\phi)_{ss}$ will be less than 0.1 mrad provided $T < 70$ sec. Since the closed loop in Fig. 5 is made up of precise computer elements, larger values of T could have been obtained (or the same e_ϕ with larger eccentricity) by adding extra compensation, such as another integrator in the open loop.

Typical values of the system parameters consistent with these bandwidth requirements are: angular frequency of rotation, $\omega_s = 10$ rad/sec; radius, $r = 0.322$ ft; moment of inertia of pendulum, $I_3 = 0.01$ slug-ft^2; spring constant of flexure pivot, $K_s = 10^{-6}$ ft-lb/rad, natural frequency $\omega_0 = (K_s/I_3)^{1/2} = 10^{-2}$ rad/sec, with damping ratio $\zeta = 0.01$; number of cycles integrated by phase error detector, $N = 100$. These values will be assumed in the subsequent error analysis.

Quantities Sensed by the Accelerometer

The preceding theoretical development was based on ideal conditions and did not consider sources of error, such as misalignments. These will now be discussed, using symbols defined in Fig. 9.

In order that a modified Lagrange equation can be easily derived, it is convenient to define a rectangular coordinate system with origin O at the true center of curvature of the flexure pivot and with unit vector $\mathbf{U}_0$ along the true axis of the pivot. Because of misalignments, O and $\mathbf{U}_0$ no longer exactly coincide with the wheel axis of rotation. Unit vector $\mathbf{U}_r$ from O is perpendicular to $\mathbf{U}_0$ and passes through the true centroid of the pendulum, so that $\mathbf{r}_c = r_c\mathbf{U}_r$. Finally, defining $\mathbf{U}_\theta = \mathbf{U}_0 \times \mathbf{U}_r$, generalized coordinate θ is defined by $d\mathbf{r}_c = r_c d\theta\mathbf{U}_\theta$ and $\dot{\mathbf{U}}_r = \dot{\theta}\mathbf{U}_\theta$, $\dot{\mathbf{U}}_\theta = -\dot{\theta}\mathbf{U}_r$. Thus, $\ddot{\mathbf{r}}_c = \ddot{r}_c\mathbf{U}_r + 2\dot{r}_c\dot{\theta}\mathbf{U}_\theta + r_c\ddot{\theta}\mathbf{U}_\theta - r_c\dot{\theta}^2\mathbf{U}_r$, which, assuming that r_c is fixed, becomes

$$\ddot{\mathbf{r}}_c = r_c\ddot{\theta}\mathbf{U}_\theta - r_c\dot{\theta}^2\mathbf{U}_r \tag{23}$$

Using Eq. (23), and introducing the disturbing torques transmitted by the flexure pivot, the Lagrange equation corresponding to idealized Eq. (21) is

$$m\delta\ddot{\mathbf{R}}_0\cdot(r_c\mathbf{U}_\theta) + I_{33} = q + K_s(\theta_W - \theta) + 2\zeta\omega_0 I_{33}(\dot{\theta}_W - \dot{\theta}) \tag{24}$$

where I_{33} is about $\mathbf{U}_0$, and $(\theta_W - \theta)$ is the deviation of the pendulum from the pivot zero torque position on the wheel. In the notation of Fig. 9,

$$\delta\ddot{\mathbf{R}}_0 = (\ddot{\mathbf{P}} - \mathbf{G}_{cm}) - \mathbf{g}_\mathbf{p} - \ddot{\mathbf{p}} \tag{25}$$

where $\mathbf{g}_\mathbf{p}$ is due to the gravitational gradient from the vehicle center of mass to point O.

The accelerometer seismic mass m^s is located by vector $\mathbf{r} = r(\mathbf{U}_r + \eta\mathbf{U}_\theta)$, where η is a small misalignment angle between vectors $\mathbf{r}$ and $\mathbf{r}_c$. In addition, the sensitive axis is defined by $\mathbf{U}_a = \mathbf{U}_\theta + \mathbf{e}$, where $\mathbf{e} = e_r\mathbf{U}_r + e_0\mathbf{U}_0$ represents a misalignment. The seismic mass satisfies $m^s\ddot{\mathbf{R}} = \mathbf{F} + m^s\mathbf{G} + \mathbf{F}^{\text{dist}}$, where $\mathbf{F}$ is the constraint force between the seismic mass and case. The accelerometer measures $a = (1/m^s)\mathbf{F}\cdot\mathbf{U}_a$. Substituting for $\mathbf{F}$ and $\mathbf{U}_a$,

$$a = (\delta\ddot{\mathbf{R}}_0 + \ddot{\mathbf{r}})\cdot\mathbf{U}_\theta + \delta\ddot{\mathbf{R}}_0\cdot\mathbf{e} + \ddot{\mathbf{r}}\cdot\mathbf{e} - (1/m^s)\mathbf{F}^{\text{dist}}\cdot\mathbf{U}_a - \mathbf{g}_\mathbf{r}\cdot\mathbf{U}_\theta - \mathbf{g}_r\cdot\mathbf{e} \tag{26}$$

where $\mathbf{g}_\mathbf{r}$ is due to the gravitational gradient from O to the seismic mass. This equation will be expanded by expressing $\ddot{\mathbf{r}}$ in terms of $\dot{\theta}$ and $\ddot{\theta}$, which can be obtained from Lagrange's equation. Proceeding as in the derivation of Eq. (23),

$$\ddot{\mathbf{r}} = r\ddot{\theta}\mathbf{U}_\theta - r\dot{\theta}^2\mathbf{U}_r - \eta r\ddot{\theta}\mathbf{U}_r + \eta r\dot{\theta}^2\mathbf{U}_\theta \tag{27}$$

Substituting Eq. (27) into Eq. (26), evaluating $\dot{\theta}$, $\ddot{\theta}$ by means of Eq. (24), and introducing transform notation,

$$\begin{aligned} a = {} & \frac{S^2[1 - (r_c r/\rho_{33}^2)(1 - \epsilon_r\eta)] + 2\zeta\omega_0 S + \omega_0^2}{S^2 + 2\zeta\omega_0 S + \omega_0^2}\{\delta\ddot{\mathbf{R}}_0\cdot\mathbf{U}_\theta\} + \\ & (1 - \epsilon_r\eta)\frac{2\zeta\omega_0 S + \omega_0^2}{S^2 + 2\zeta\omega_0 S + \omega_0^2}\{r\ddot{\theta}_w\} + \\ & \frac{S^2}{S^2 + 2\zeta\omega_0 S + \omega_0^2}\frac{(I_1 - I_2)}{I_3}\{\mathbf{g}_\mathbf{r}\cdot\mathbf{U}_\theta\} + \\ & e_r\{\delta\ddot{\mathbf{R}}_0\cdot\mathbf{U}_r\} + e_0\{\delta\ddot{\mathbf{R}}_0\cdot\mathbf{U}_0\} - \\ & (e_r + \eta)\left[\{r\omega_s^2\} + \frac{\omega_0 S}{S^2 + \zeta\omega_0 S + \omega_0^2}\left\{\frac{\omega_s}{\omega_0}\delta\ddot{\mathbf{R}}_0\cdot\mathbf{U}_\theta\right\}\right] - \\ & \left\{\frac{1}{m^s}\mathbf{F}^{\text{dist}}\cdot\mathbf{U}_a\right\} - \{\mathbf{g}_r\cdot\mathbf{U}_\theta\} - \{\mathbf{g}_r\cdot\mathbf{e}\} \end{aligned} \tag{28}$$

Equation (28) shows the quantities actually sensed by the accelerometer which can be compared with idealized Eq. (22). There are ten terms, each of whose origin can be identified by the factor in braces, { }. The first term $\{\delta\ddot{\mathbf{R}}_0\cdot\mathbf{U}_\theta\}$ represents the effect of disturbing accelerations at 0, modified by the dynamics of the flexure pivot and pendulum. The

second term $\{r\ddot{\theta}_w\}$ represents the effect of speed variations of the wheel which are coupled to the pendulum through the pivot. The third term $\{\mathbf{g}_r \cdot \mathbf{U}_\theta\}$ represents gravitational gradient torques on the pendulum when its principle moments I_1, I_2 are not exactly equal. The fourth and fifth terms $\{\delta\ddot{\mathbf{R}}_0 \cdot \mathbf{U}_r\}$, $\{\delta\ddot{\mathbf{R}}_0 \cdot \mathbf{U}_0\}$ represent imperfect isolation of the accelerometer from disturbance accelerations because of sensitive axis misalignments with the pivot. The sixth and seventh terms represent pickup of centripetal acceleration due to sensitive axis misalignment from the tangent direction: the sixth term $\{r\omega_s^2\}$ shows the effect of centripetal acceleration due to the wheel rotation frequency ω_s, whereas the seventh term $\{(\omega_s/\omega_0)\delta\ddot{\mathbf{R}}_0 \cdot \mathbf{U}_\theta\}$ shows the additional effect of rotation rate of the pendulum with respect to the wheel. The wheel speed variations do not appear, since their effect is of higher order when $\omega_0 \ll \omega_s$. The eighth term $\{(1/m^s)\mathbf{F}^{\text{dist}} \cdot \mathbf{U}_a\}$ represents gravitational attraction from nearby masses in the vehicle. Finally, the ninth and tenth terms $\{\mathbf{g}_r \cdot \mathbf{U}_\theta\}$, $\{\mathbf{g}_r \cdot \mathbf{e}\}$ represent, respectively, the desired gravitational gradient signal g_θ, and pickup of the undesired gravitational gradient signals g_r, g_0 [Eq. (4)] because of sensitive axis misalignment.

Magnitude of Errors

The magnitude of the error sources in Eq. (28) will now be compared with the magnitude of the desired signal g_θ. For the system parameters selected, $|g_\theta| = 1.61 \cdot 10^{-8}\, g$.

The ability of the flexure pivot to isolate the accelerometer from disturbances is indicated by the transfer functions in Eq. (28) which attenuate undesired signals near the desired signal frequency $2\omega' = 2\omega_s$, since $\omega_0 \ll \omega_s$. Other sources of error appear with factors e_r, e_0, η, $[1 - (r_c r/\rho_{33}^2)]$, $(I_1 - I_2)/I_3$, which represent misalignments and dimensional errors. By careful design, these factors can be reduced to 10^{-4} or less.

After these reduced quantities are sensed by the accelerometer, the phase error detector further attenuates all signals except those at frequencies very near $2\omega'$, as indicated in Fig. 6. In particular, many sources of error appear at zero frequency or frequency ω' because of dot products with rotating vectors $\mathbf{U}_\theta$, $\mathbf{U}_r$. It can be shown that such signals are attenuated by $1/N \cdot \delta T_s/T_s$, where $\delta T_s/2\pi T_s$ is the angular deviation of the sampling switch from its nominal position on the wheel. Since the switch is fixed, $\delta T_s/T_s$ should be of order 10^{-4} or less, so that the net attenuation is of the order 10^{-6}. Signals with frequencies which differ from 0 or ω' by an amount $\Delta\omega$ will only be attenuated by $\Delta\omega/\omega'$. But the phase error detector will shift these frequencies to frequencies ω' or higher, while the desired signal is shifted to zero frequency. These signals can then be further attenuated by notch filters in the phase tracking loop of Fig. 5, since the required loop bandwidth is much lower than ω'. Undesired signals due to resolver errors and accelerometer scale errors will occur at frequencies $4\omega'$, $8\omega'$, . . ., and will be similarly attenuated by the phase error detection and notch filters.

The disturbance acceleration $\delta\ddot{\mathbf{R}}_0$, which appears in several terms of Eq. (28), consists of the three components defined in Eq. (25). Because of drag or thrust acceleration, the component $(\ddot{\mathbf{P}} - \mathbf{G}_{cm})$ may be as large as $10^{-3}\, g$ and introduces signals at frequencies near ω' and zero which are attenuated to $10^{-7}\, g$ in Eq. (28). These signals are further attenuated to negligible values in the phase error detector and tracking loop. Similarly, $\mathbf{g}_\mathbf{p}$ is of the order $10^{-7}\, g$ for 1-ft displacement of O from the vehicle cm and is finally attenuated to negligible values. The third term $\ddot{\mathbf{p}}$ will introduce signals at frequencies near ω' and zero because of slow angular motions of the vehicle and wheel unbalance or misalignment of O with the axis of wheel rotation. Again, these signals will be attenuated to negligible values.

The largest terms in Eq. (28) will result from wheel speed variations $\{r\ddot{\theta}_w\}$ and pickup of centripetal acceleration $\{r\omega_s^2\}$ due to sensitive axis misalignments. At frequencies near $2\omega'$,

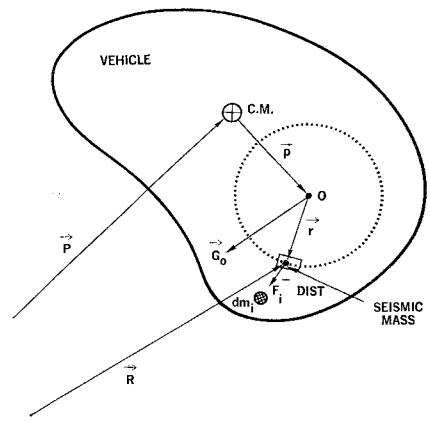

Fig. 9 Definition of quantities in error analysis.

wheel speed variations are attenuated by 10^{-5} because of the flexure pivot. However, slow variations at frequencies less than ω_0 will not be attenuated. Such variations may have magnitudes of the order $10^{-4}\, g$. Also, a sensitive axis misalignment $e_r = 10^{-4}$ will produce a d.c. signal of magnitude $10^{-4}\, g$ due to centripetal acceleration. Finally, accelerometer bias drift may be as large as $10^{-4}\, g$ at near zero frequency. The phase error detector and notch filters in the phase tracking loop should attenuate such errors to negligible values. Furthermore, d.c. errors detected by the accelerometer can be identified at the output of the phase error detector, since they appear at frequency $2\omega'$. This information could be fed back in an "adaptive" manner to bias out such errors before they enter the accelerometer.

Signals that occur at frequency $2\omega'$ will not be attenuated. This category consists of the gravitational gradient signals. But the undesired components g_r, g_0 will be picked up with magnitudes 10^{-4} times that of the desired signal g_θ because of the factors e_r, e_0, $(I_1 - I_2)/I_3$, and they will not cause significant errors. The term due to local mass attraction will also have a component at frequency $2\omega'$. For a mass dm at distance ρ from 0, at an angle ψ from the plane of rotation, this component has a magnitude

$$|\Delta g_\theta| = 3k\, dm/\rho^3 \cdot r/2(1 + \sin^2\psi)$$

If dm is a 1-lb mass at $\rho = 1$ ft with $\psi = 0$, then $|\Delta g^\theta| = 1.60 \times 10^{-11}\, g$, which can cause a phase error of 1 mil. Such errors would become excessive unless they were precalculated as functions of vehicle mass distribution and biased out. Similar errors would arise because of electrical pickup in the rotating windings. Again, such errors can be reduced by careful design and biasing.

The foregoing discussion makes it clear that the most critical sources of error are those with a continuous power spectrum near frequency $2\omega'$, since such errors cannot be filtered from the phase tracking loop. Such errors arise because of random vibrations of point O, as represented by $\ddot{\mathbf{p}}$ and random angular wheel speed variations $\ddot{\theta}_w$. From Eq. (28), these disturbances are attenuated by 10^{-4} and 10^{-5}, respectively, before being sensed by the accelerometer. They are then combined with random accelerometer noise to yield a total noise power spectrum $\Phi_N(\omega)$ out of the accelerometer. As shown in Eq. (2) and Fig. 6, the phase error detector passes such noise in a very narrow band of frequencies centered at the desired signal frequency $2\omega'$. This bandwidth is the bandwidth ω_{BW} required of the phase tracking loop in following the vertical. The resultant error in the vertical is $(P_{\text{out}}/P_{\text{sig}})^{1/2}$ where

$$P_{\text{out}}/P_{\text{sig}} = \omega_{BW}\Phi_N(2\omega')/|g_\theta|^2 \qquad (29)$$

The feasibility and ultimate accuracy of the instrument will therefore depend on whether a suspension system and

accelerometer can be designed with sufficiently low noise power spectrum at some frequency $2\omega'$.

References

[1] Oberth, H., "A precise attitude control for artificial satellites," *Vistas in Astronautics* (Pergamon Press, London, 1958), Vol. 1, pp. 217–255.

[2] Crowley, J. C., Kolodkin, S. S., and Schneider, A. M., "Some properties of the gravitation field and their possible application to space navigation," Inst. Radio Engrs. Trans. on Space Electron. Telemetry **SET-5**, 47–54 (March 1959).

[3] Roberson, R. E. (ed.), "Sensing and actuation methods," Methods for the Control of Satellites and Space Vehicles, Vol. I, Wright Air Development Div. TR 60-643 (July 31, 1960).

[4] Roberson, R. E., "Gravity gradient determination of the vertical," ARS J. **31**, 1509–1515 (1961).

[5] Diesel, J. W., "A new navigation concept for orbital systems, spacecraft, and intercontinental missiles," TM 61-34, Litton Systems, Inc. (November 1, 1961).

[6] Blazek, H. F., "Feasibility and design of the rotating pendulous accelerometer," AIAA Preprint 63-317 (August 1963).

[7] Roberson, R. E. and Tatistcheff, D., "The potential energy of a small rigid body in the gravitational field of an oblate spheroid," J. Franklin Inst. **262**, 209–214 (1956).

[8] Roberson, R. E., "Gravitational torque on a satellite vehicle," J. Franklin Inst. **264**, 13–22 (January 1958)

[9] Goldstein, H., *Classical Mechanics* (Addison-Wesley Publishing Co., Inc., Reading, Mass., 1959), Chaps. 1–5.

JULY 1964 AIAA JOURNAL VOL. 2, NO. 7

Optimum Low-Thrust Rendezvous and Station Keeping

THEODORE N. EDELBAUM*

United Aircraft Corporation, East Hartford, Conn.

Analytic solutions are determined for the optimum correction of all six elements of elliptic satellite orbits with low-thrust, power-limited propulsion systems. The optimum direction and magnitude of thrust are determined as functions of time so as to minimize the fuel required to rendezvous in a given time or to minimize the fuel required for station keeping in the presence of known perturbations. The motion of the vehicle under the action of the optimum thrust program is also determined analytically. The solutions obtained are divided into two classes, depending on whether rendezvous requires few or many revolutions. In the latter case, simple analytic solutions are obtained explicitly by neglecting short-period perturbations.

Nomenclature

a	=	semimajor axis
A	=	thrust acceleration magnitude
A_T	=	circumferential component of thrust acceleration
A_R	=	radial component of thrust acceleration
A_W	=	normal component of thrust acceleration
e	=	eccentricity
E	=	eccentric anomaly
F	=	variational Hamiltonian
J	=	defined by Eq. (1)
K	=	gravitational constant
$L, M, \ldots, U$	=	functions defined following Eq. (7)
M	=	mean anomaly
t	=	time
λ	=	Lagrange multiplier
θ_1	=	small rotation of major axis in orbit plane
θ_2	=	small rotation of orbit plane around major axis
θ_3	=	small rotation of orbit plane around latus rectum

Introduction

THE present paper is one of a series of papers[1–4] containing analytic solutions for optimum low-thrust power-limited trajectories in inverse-square force fields. The previous papers in this series have considered long-time transfer between arbitrary circular orbits,[1] long-time escape from elliptic orbits,[2] long-time transfer between coplanar circular and elliptic orbits,[3] and transfer between close circular orbits.[4]

Presented as Preprint 63-154 at the AIAA Summer Meeting, Los Angeles, Calif., June 17–20, 1963. The author would like to thank Edward K. Blum of Wesleyan University for clarifying and correcting an early draft of the derivations contained herein.

* Senior Research Engineer, Research Laboratories. Associate Fellow Member AIAA.

The propulsion system that effects the changes of the elliptic orbit is assumed to be power-limited, i.e., it operates at constant exhaust power with a thrust magnitude inversely proportional to the exhaust velocity.[5,6] The direction and magnitude of the thrust, which is assumed to be completely variable, is to be determined as a function of time so as to minimize fuel consumption.

There have been a number of previous studies of trajectory optimization for power-limited propulsion systems; some of the more important studies are contained in Refs. 5–13. Most of these studies are concerned with numerical results for inverse-square force fields.[5–11] Reference 12 obtains analytic solutions for optimum trajectories in field-free space, whereas Ref. 13 obtains analytic solutions for the optimum thrust programs for small changes of five elements of an elliptic orbit in an inverse-square field. The present paper extends the work of Ref. 13 to obtain the optimum thrust program for small changes of all six elements and to determine the optimal motion of the vehicle and the fuel consumption under the action of this thrust program.

Assumptions

The analyses of this paper are carried out under the assumption that the perturbations due to thrust of all the elements of an elliptic orbit are small and that the thrust acceleration A is small compared to the acceleration of gravity. The other assumptions are an inverse-square force field and a variable-thrust powerplant operating at constant exhaust power with no bounds on the thrust magnitude or direction.

Derivation

The derivation is carried out using a formulation of the problem of Bolza similar to that of Breakwell[14] and of Pon-